



Nanoscale Friction Varied by Isotopic Shifting of Surface Vibrational Frequencies

Rachel J. Cannara, *et al.*

Science **318**, 780 (2007);

DOI: 10.1126/science.1147550

The following resources related to this article are available online at www.sciencemag.org (this information is current as of June 3, 2008):

Updated information and services, including high-resolution figures, can be found in the online version of this article at:

<http://www.sciencemag.org/cgi/content/full/318/5851/780>

Supporting Online Material can be found at:

<http://www.sciencemag.org/cgi/content/full/318/5851/780/DC1>

This article **cites 32 articles**, 2 of which can be accessed for free:

<http://www.sciencemag.org/cgi/content/full/318/5851/780#otherarticles>

This article has been **cited by** 2 article(s) on the ISI Web of Science.

This article appears in the following **subject collections**:

Physics, Applied

http://www.sciencemag.org/cgi/collection/app_physics

Information about obtaining **reprints** of this article or about obtaining **permission to reproduce this article** in whole or in part can be found at:

<http://www.sciencemag.org/about/permissions.dtl>

References and Notes

- J. M. Cordes, T. J. W. Lazio, M. A. McLaughlin, *N. Astron. Rev.* **48**, 1459 (2004).
- B. M. S. Hansen, M. Lyutikov, *Mon. Not. R. Astron. Soc.* **322**, 695 (2001).
- M. J. Rees, *Nature* **266**, 333 (1977).
- M. A. McLaughlin *et al.*, *Nature* **439**, 817 (2006).
- R. N. Manchester, G. Fan, A. G. Lyne, V. M. Kaspi, F. Crawford, *Astrophys. J.* **649**, 235 (2006).
- L. Staveley-Smith *et al.*, *Proc. Astron. Soc. Pac.* **13**, 243 (1996).
- J. M. Cordes, M. A. McLaughlin, *Astrophys. J.* **596**, 1142 (2003).
- D. R. Lorimer, M. Kramer, *Handbook of Pulsar Astronomy* (Cambridge Univ. Press, Cambridge, 2005).
- L. C. Lee, J. R. Jokipii, *Astrophys. J.* **206**, 735 (1976).
- J. M. Cordes, T. J. W. Lazio, <http://arxiv.org/abs/astro-ph/0207156> (2002).
- R. W. Hilditch, I. D. Howarth, T. J. Harries, *Mon. Not. R. Astron. Soc.* **357**, 304 (2005).
- K. Hurley *et al.*, *Astrophys. J. Suppl. Ser.* **164**, 124 (2006).
- K. Hurley, personal communication.
- G. Paturel *et al.*, *Astron. Astrophys.* **412**, 45 (2003).
- K. Ioka, *Astrophys. J.* **598**, L79 (2003).
- S. Inoue, *Mon. Not. R. Astron. Soc.* **348**, 999 (2004).
- P. R. Maloney, J. Bland-Hawthorn, *Astrophys. J.* **522**, L81 (1999).
- J. M. Cordes, N. D. R. Bhat, T. H. Hankins, M. A. McLaughlin, J. Kern, *Astrophys. J.* **612**, 375 (2004).
- V. Kalogera *et al.*, *Astrophys. J.* **601**, L179 (2004).
- D. Guetta, M. Della Valle, *Astrophys. J.* **657**, L73 (2007).
- P. Madau, M. Della Valle, N. Panagia, *Mon. Not. R. Astron. Soc.* **297**, L17 (1998).
- J.-P. Macquart, *Astrophys. J.* **658**, L1 (2007).
- R. N. Manchester *et al.*, *Mon. Not. R. Astron. Soc.* **328**, 17 (2001).
- R. T. Edwards, M. Bailes, W. van Straten, M. C. Britton, *Mon. Not. R. Astron. Soc.* **326**, 358 (2001).
- M. Burgay *et al.*, *Mon. Not. R. Astron. Soc.* **368**, 283 (2006).
- B. A. Jacoby, M. Bailes, S. M. Ord, H. S. Knight, A. W. Hotan, *Astrophys. J.* **656**, 408 (2007).
- S. W. Amy, M. I. Large, A. E. Vaughan, *Proc. Astron. Soc. Aust.* **8**, 172 (1989).
- B. W. Stappers, A. G. J. van Leeuwen, M. Kramer, D. Stinebring, J. Hessels, in *Proceedings of the 363. Heraeus Seminar on Neutron Stars and Pulsars*, W. Becker, H. H. Huang, Eds. (Physikzentrum, Bad Honnef, Germany, 2006), pp. 101–103.
- V. L. Ginzburg, *Nature* **246**, 415 (1973).
- S. Johnston *et al.*, *ATNF SKA Memo 13* (Australia Telescope National Facility, 2007).
- P. N. Wilkinson, K. I. Kellermann, R. D. Ekers, J. M. Cordes, T. J. W. Lazio, *N. Astron. Rev.* **48**, 1551 (2004).
- J. E. Gaustad, P. R. McCullough, W. Rosing, D. Van Buren, *Proc. Astron. Soc. Pac.* **113**, 1326 (2001).
- S. Stanimirović, L. Staveley-Smith, J. M. Dickey, R. J. Sault, S. L. Snowden, *Mon. Not. R. Astron. Soc.* **302**, 417 (1999).
- The Parkes Radio Telescope is part of the Australia Telescope, which is funded by the Commonwealth of Australia for operation as a National Facility managed by the Commonwealth Scientific and Industrial Research Organisation. We thank R. Manchester for making the archival data available to us. This research has made use of data obtained from the High Energy Astrophysics Science Archive Research Center, provided by NASA's Goddard Space Flight Center. We thank K. Hurley for providing access to the GCN network archive, and V. Kondratiev, S. Tingay, S. Johnston, F. Camilo, and J. Bland-Hawthorn for useful comments on the manuscript. We acknowledge the prompt awarding of follow-up time by the ATNF Director and thank L. Toomey and P. Sullivan for observing assistance.

Supporting Online Material

www.sciencemag.org/cgi/content/full/1147532/DC1
Materials and Methods
Figs. S1 and S2
References

9 July 2007; accepted 20 September 2007
Published online 27 September 2007;
10.1126/science.1147532
Include this information when citing this paper.

Nanoscale Friction Varied by Isotopic Shifting of Surface Vibrational Frequencies

Rachel J. Cannara,^{1*} Matthew J. Brukman,^{2†} Katherine Cimatú,³ Anirudha V. Sumant,^{2‡} Steven Baldelli,³ Robert W. Carpick^{2§}

Friction converts kinetic energy at sliding interfaces into lattice vibrations, but the detailed mechanisms of this process remain unresolved. Atomic force microscopy measurements reveal that changing the mass of the terminating atoms on a surface, and thus their vibrational frequencies, affects nanoscale friction substantially. We compared hydrogen- and deuterium-terminated single-crystal diamond and silicon surfaces, and in all cases the hydrogenated surface exhibited higher friction. This result implies that the lower natural frequency of chemisorbed deuterium reduces the rate at which the tip's kinetic energy is dissipated. This discovery is consistent with a model describing energy transfer to adsorbates from a moving surface.

Friction converts translational kinetic energy to vibrational energy. Hence, rubbing two bodies together produces heat. This process occurs even in the absence of wear. In contact-mode atomic force microscopy (AFM),

a nanoscale tip slides along a surface, but based on theories of atomic dissipation, some of the tip's translational energy can be converted to lattice vibrations or electronic carriers (1–4). It would be technologically beneficial to control how energy is lost through each of these channels by tuning phononic or electronic properties. Recently, Park *et al.* increased nanoscale friction electronically (5), whereas in the present work we show that friction also depends on the vibrational properties of surfaces.

We altered surfaces by varying the mass, but not the chemistry, of the chemisorbed terminating surface atom. Leaving the surface chemistry unchanged avoids chemical effects due to different interfacial forces. Based on a model of phononic dissipation for friction (6), the surface monolayer acts as an energy-transfer medium, absorbing kinetic energy from the tip

at rates dependent on the adsorbates' natural vibration frequencies (Fig. 1). Because lighter atoms vibrate faster, energy dissipation should be more rapid, and therefore friction should be greater than friction produced by heavier species.

The systems most likely to exhibit observable mass contrast are hydrogen (H)– and deuterium (D)–terminated surfaces, the most durable and inert of which is diamond (7). H- and D-terminated silicon (Si) surfaces are less stable (the surface oxidizes in air after 1 or 2 hours) (8), but studying Si provides an additional test and provides information on an important ma-

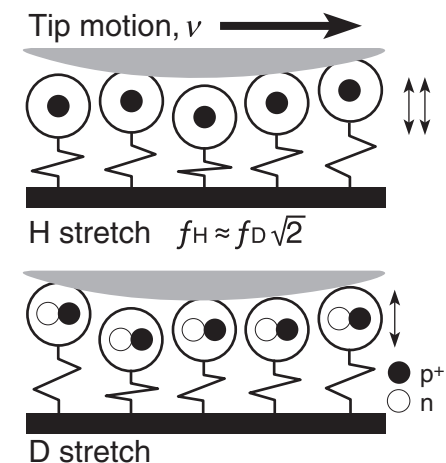


Fig. 1. A schematic of the frictional interface. Vibrating adsorbates collide with and dissipate kinetic energy from the moving tip at a rate that depends on the adsorbate's frequency and thus its mass; that is, at different rates for H than for D.

¹Department of Physics, University of Wisconsin–Madison, Madison, WI 53706, USA. ²Department of Engineering Physics, University of Wisconsin–Madison, Madison, WI 53706, USA. ³Department of Chemistry, University of Houston, Houston, TX 77004, USA.

*Present address: IBM Research GmbH, Zurich Research Laboratory, 8803 Rüschlikon, Switzerland.

†Present address: Department of Materials Science and Engineering, University of Pennsylvania, Philadelphia, PA 19104, USA.

‡Present address: Center for Nanoscale Materials, Argonne National Laboratory, Argonne, IL 60439, USA.

§Present address: Department of Mechanical Engineering and Applied Mechanics, University of Pennsylvania, Philadelphia, PA 19104, USA.

terial for nanoscale devices and systems. H-terminated diamond also exhibits distinctive electronic properties that depend on the concentration of surface physisorbed contaminants. As described in the supporting online material (9), the absorption of ambient hydrocarbons does indeed change friction for diamond.

The vibrational frequency ω of an adsorbed atom is determined by its mass, the mass of the substrate atom(s) to which it is bonded, and the bond stiffness k . In particular, $\omega = \sqrt{k/\mu}$, where μ is the reduced mass of the bonded adsorbate. In the limit of heavy substrate atoms, μ is approximately the adsorbate's mass, m . On diamond, the ratio of the vibrational frequency of H (ω_H) compared to D (ω_D) is $\omega_H/\omega_D = \sqrt{\mu_D/\mu_H} = 1.363$ (10, 11). On Si(111), the ratio is 1.389 (12–14).

Diamond(001) single-crystal surfaces were terminated with H or D monolayers by means of a hot-filament process (9). This procedure formed well-ordered nearly saturated surfaces, as demonstrated by sum frequency generation (SFG) spectroscopy (Fig. 2A). Vibrational assignments were made on the basis of reported values (15–19). Full coverage of H was achieved, based on the position and intensity of the C-H stretching peak measured at 2835 cm^{-1} on a C(111) surface that was terminated simultaneously with the C(001)-H surface. The peak at 2930 cm^{-1} is assigned to the H-terminated C(001)-(2 \times 1) reconstruction (20). On the deuterated sample, a

single peak at 2160 cm^{-1} was observed, corresponding to the C-D stretch. Analysis of the CH region from 2750 to 3150 cm^{-1} showed no features significantly above the background, demonstrating full coverage by D and a lack of contamination or residual H.

The friction force F_f was measured on diamond as a function of load in both dry nitrogen and ultrahigh vacuum (UHV), alternating multiple times between the H- and D-terminated samples in each case. The same hydrocarbon (HC)-coated tip was used for these experiments. The friction versus load data were fit to a continuum model for the contact area A using the model of interfacial friction $F_f = \tau_0 A$, where τ_0 is the interfacial shear strength (21), a model appropriate in the absence of wear and for load-independent shear strengths. We fit the friction data with a continuum mechanics model describing the dependence of A on load, assuming a spherical, elastic, adhesive contact (22, 23). This model eliminates the need to make any assumptions about the spatial extent of adhesion or the relation between pull-off forces and the work of adhesion.

Caution should be used when applying continuum mechanics to nanoscale contacts, as indicated by recent molecular dynamics simulations (24, 25). Whatever corrections were required, our use of the same tip, substrate, and environment for all H versus D comparisons on diamond, and separately on Si, allowed us to determine unambiguously whether an isotopic substitution effect occurred.

From the continuum mechanics fits, we extracted effective shear strengths (\bar{C}) and work-of-adhesion (γ) values. \bar{C} is proportional to τ_0 , normalized by the appropriate power of the elastic contact modulus (9, 26, 27), which eliminates any dependence on the unknown but constant elastic properties of the tip. Absolute shear strengths (τ_0) were also estimated by selecting reasonable values for the elastic constants of the tip (9), but the effective shear strengths were sufficient for the analysis, because the same tip was always used to compare H- and D-terminated pairs.

The results are summarized in Table 1. Representative plots of \bar{C} for the two terminations and environments studied are shown in Fig. 2B. These data are friction measurements divided by their respective contact area fits at each load, indicating the difference between C-H and C-D beyond the residuals. Deviations at low loads arise from fitting errors intrinsic to the small, steeply changing contact area. The shear strengths (effective and absolute) were an average of 1.26 ± 0.05 and 1.26 ± 0.07 times greater for the H-terminated surfaces for N_2 and UHV, respectively.

Single-crystal Si(111) samples were terminated by H or D by means of an established wet etch process (9), the quality of which was verified by contact angle and x-ray photoelectron spectroscopy measurements. Friction versus load measurements on H- and D-terminated Si(111) samples were obtained in dry N_2 with the same silicon nitride tip. Atomic mass contrast was again observed (Fig. 3 and Table 1), with shear

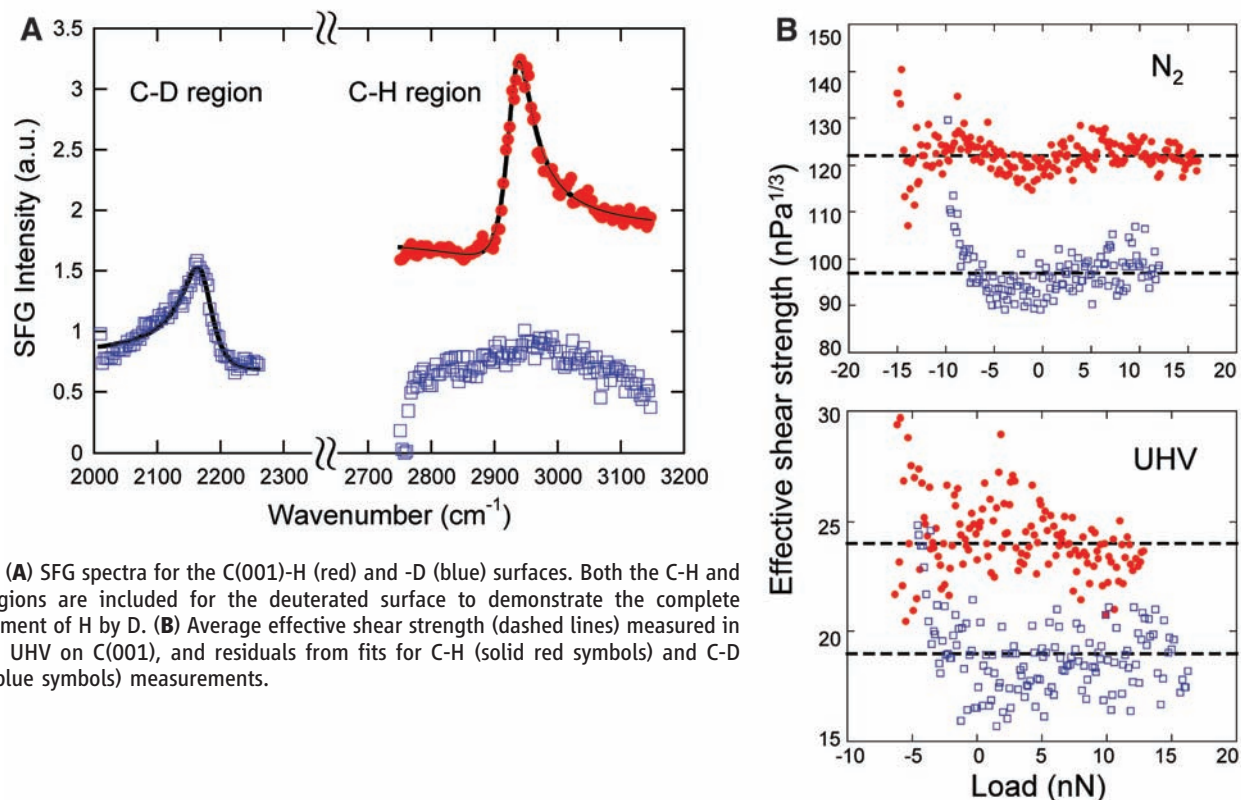


Fig. 2. (A) SFG spectra for the C(001)-H (red) and -D (blue) surfaces. Both the C-H and C-D regions are included for the deuterated surface to demonstrate the complete replacement of H by D. (B) Average effective shear strength (dashed lines) measured in N_2 and UHV on C(001), and residuals from fits for C-H (solid red symbols) and C-D (open blue symbols) measurements.

strengths greater on the H-terminated surface according to the ratio 1.30 ± 0.09 .

The C(001)-H- and -D surfaces have nearly indistinguishable work-of-adhesion values in UHV, consistent with the expected lack of chemical contrast. The work-of-adhesion values are in the range of pure van der Waals interactions (28, 29), particularly for the UHV measurements, and display an impressively small deviation ($<7\%$), which is only expected for well-prepared surfaces in stable environments.

We claim that there is no inherent chemical contrast between the H- and D-terminated surfaces. The small interaction effect from the isotopic substitution of H with D, which can have consequences for very-long-chain polymer systems (30), is calculated to be infinitesimally small here (31). The differences in adhesion that we do observe between H- and D-terminated samples (Table 1) do not vary systematically: Adhesion is higher for H on C(001) in N_2 , lower for H on Si(111) in N_2 , and nearly indistinguishable for C(001) in UHV. The larger variations in N_2 as compared with UHV are probably due to varying degrees of contamination from ambient exposure. We also emphasize that any influence on friction by the contact area (induced by changes in adhesion) has been removed by finding the effective shear strengths.

There are no existing theoretical treatments that permit direct comparison with these experiments.

However, Persson (6) has modeled phononic friction for an adsorbate monolayer interacting with a single moving surface. Friction arises from inelastic collisions between vibrating adsorbates and the surface. Although this situation does not correspond directly to an AFM measurement where confined atoms are chemisorbed to one surface and interact with the other moving surface under load, we use the model to predict the qualitative behavior. The AFM tip takes the place of the moving surface, and the H (D) atoms correspond to the adsorbates, which are now chemisorbed to the diamond or Si substrate (as opposed to being otherwise unbonded in the model) and are assumed to be uncoupled from one another. In the theory, the friction force from vibrational damping by one adsorbate is

$$F_{f,vib}^{atom} = -m_{tip}\eta v \quad (1)$$

where m_{tip} is the dynamical effective mass of the tip, η is the damping constant of the interaction, and v is the relative sliding velocity between the tip and sample. The minus sign (excluded henceforth) indicates that the friction force opposes the direction of motion. The number of adsorbates involved is proportional to the adsorbate areal density σ and the contact area A . When any variation of η caused by non-uniform contact stresses is neglected, the total vibrational contribution will be $F_{f,vib} = m_{tip}\eta\sigma A$.

For interfacial friction, the vibrational contribution to the shear strength will be

$$\tau_{o,vib} = m_{tip}\eta\sigma v \quad (2)$$

The damping constant η is related to the density ρ and the transverse sound velocity c_T of the moving surface by

$$\eta \approx 3m\omega^4/8\pi\rho c_T^3 \quad (3)$$

where m and ω refer to the adsorbate's mass and vibrational frequency, respectively [equations 18 and 22 in (32)].

To illustrate the physics behind Eq. 3, consider an adsorbate vibrating with energy E and colliding with the moving surface (the AFM tip). During one vibration cycle, the adsorbate transfers energy $\Delta E = (m/M_S)E$ from the tip, where M_S is the mass of the portion of the tip effectively involved in the collision (33). Thus, the energy transfer rate may be expressed by $\dot{E} = -\frac{\omega}{2\pi} \left(\frac{m}{M_S}\right) E$. In the collision time $t \approx 2\pi/\omega$, a local displacement field forms in the tip within a distance c_T/ω that corresponds to a volume $(c_T/\omega)^3$. Thus, $M_S \approx \rho(c_T/\omega)^3$. The energy transfer rate is then

$$\dot{E} \approx -\frac{m\omega^4}{2\pi\rho c_T^3} E \quad (4)$$

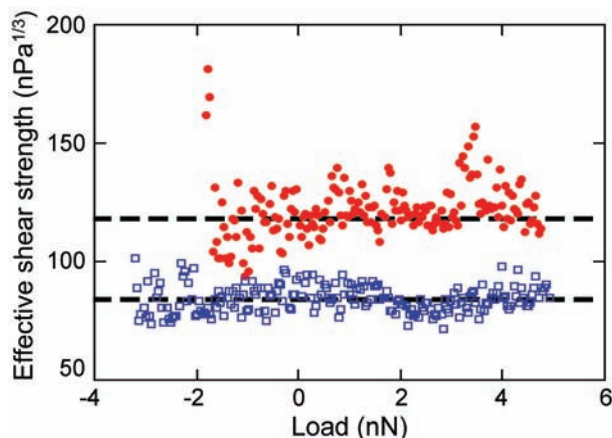
The solution to Eq. 4 is an exponential decay with damping constant $\eta = (m\omega^4)/(2\pi\rho c_T^3)$, similar to the more precisely derived quantity in Eq. 2 (6). Because $\omega \propto \mu^{-1/2}$, η , τ_o , and F_f all scale as $m/\mu^2 \approx 1/m$.

It is important to understand how damping leads to friction at the tip/sample interface. Sliding friction is caused by the loss of tip momentum to surface atoms. Atoms excited by the tip can transfer some of their energy back to the tip and help it slip to the next position. This is similar to the concept of reduced friction with increasing temperature (34). [Sørensen *et al.* (35) observed this effect of localized excitations in molecular dynamics simulations.] When the surface potential is symmetric, these excited surface atoms kick the tip in the forward and backward directions, equally promoting and opposing the tip's motion. Cantilever twist adds a bias to the otherwise symmetric potential and lowers the energy well along the sliding direction (36). Consequently, the momentum transferred back to the tip by surface atoms is more effective in the forward direction, and surface atoms can help push the tip forward. The available energy to do so is reduced by the energy lost from surface atoms to the substrate (that is, damping). Hence, although the rate of excitation vis-à-vis the tip and surface may be governed by the attempt frequencies of the surface atoms, the damping constants represent the diminished ability to transfer energy back to the tip. All of our energy transfer arguments are supported by molecular dynamics simulations, which have

Table 1. Results for measurements on diamond and Si: the work of adhesion (γ), effective (\tilde{C}) and estimated (τ_o) shear strengths, and their ratio (τ_H/τ_D). The effective shear strength is calculated from the Carpick-Ogletree-Salmeron (COS) transition fits (9, 23). Uncertainties correspond to the standard error on the mean, neglecting systematic uncertainties.

Surface, tip material, environment	Adsorbate	γ (mJ/m ²)	\tilde{C} (nPa ^{1/3})	τ_o (MPa)	τ_H/τ_D
C(001), HC-coated, N ₂	H	56 ± 2	122 ± 2	1010 ± 17	1.26 ± 0.05
	D	41 ± 2	97 ± 5	806 ± 38	
C(001), HC-coated, UHV	H	30 ± 2	24 ± 1	202 ± 11	1.26 ± 0.07
	D	25 ± 1	19 ± 1	161 ± 7	
Si(111), Si ₃ N ₄ -coated, N ₂	H	113 ± 7	111 ± 7	680 ± 40	1.30 ± 0.09
	D	169 ± 3	86 ± 4	530 ± 20	

Fig. 3. Average effective shear strength (dashed lines) on Si(111) and residuals from representative fits for the Si-H (solid red symbols) and Si-D (open blue symbols) measurements.



observed H atoms to act as an energy transfer medium to the bulk, specifically for diamond surfaces in sliding contact (37).

This damping model predicts $F_{f,vib}^H/F_{f,vib}^D \approx 1.72$ for diamond and $F_{f,vib}^H/F_{f,vib}^D \approx 1.86$ for Si. Other additive, mass-independent contributions to friction beyond this phononic mechanism will reduce the measured ratios from the theoretical predictions, as observed (Table 1). The predicted ~8% difference in $F_{f,vib}^H/F_{f,vib}^D$ for diamond versus Si is within our experimental uncertainty and may also be counteracted by the increased coupling of surface vibrational modes of deuterated Si(111) to bulk phonons (13) as compared with hydrogenated Si(111) (12). On diamond, surface modes overlap much less with bulk phonons (11). Furthermore, relaxing the assumption that the adsorbates are uncoupled (that is, considering coupled delocalized vibrations) leads to a weaker predicted mass contrast (32). It is likely, however, that surface defects, which accentuate the effect of localized vibrations (9), are present and may even be the dominating contribution to dissipation.

References and Notes

- M. Cieplak, E. D. Smith, M. O. Robbins, *Science* **265**, 1209 (1994).
- C. Mak, C. Daly, J. Krim, *Thin Sol. Films* **253**, 190 (1994).
- B. N. J. Persson, A. I. Volokitin, *J. Chem. Phys.* **103**, 8679 (1995).
- J. B. Sokoloff, *Phys. Rev. B* **52**, 5318 (1995).
- J. Y. Park, D. F. Ogletree, P. A. Thiel, M. Salmeron, *Science* **313**, 186 (2006).
- B. N. J. Persson, *Sliding Friction: Physical Principles and Applications* (Springer, Berlin, ed. 2, 2000), pp. 182–183.
- T. Ando, M. Ishii, M. Kamo, Y. Sato, *Diam. Rel. Mater.* **4**, 607 (1995).
- S. Ye *et al.*, *Surf. Sci.* **476**, 121 (2001).
- Supporting material is available on Science Online.
- A. Glebov, J. P. Toennies, S. Vollmer, S. A. Safron, J. G. Skofronick, *Phys. Rev. B* **57**, 10082 (1998).
- S. Thachepan *et al.*, *Phys. Rev. B* **68**, 041401(R) (2003).
- B. Sandfort, A. Mazur, J. Pollman, *Phys. Rev. B* **51**, 7139 (1995).
- V. Gräschus, A. Mazur, J. Pollman, *Surf. Sci.* **368**, 179 (1996).
- C. Stuhlmann, G. Bogdányi, H. Ibach, *Phys. Rev. B* **45**, 6786 (1992).
- H.-C. Chang, J.-C. Lin, J.-Y. Wu, K.-H. Chen, *J. Phys. Chem.* **99**, 11081 (1995).
- C. L. Cheng, J. C. Lin, H. C. Chang, J. K. Wang, *J. Chem. Phys.* **105**, 8977 (1996).
- T. Anzai *et al.*, *J. Mol. Struct.* **352–353**, 455 (1995).
- R. P. Chin, J. Y. Huang, Y. R. Shen, T. J. Chuang, H. Seki, *Phys. Rev. B* **52**, 5985 (1995).
- R. P. Chin *et al.*, *Phys. Rev. B* **45**, 1522 (1992).
- L. V. Zhigilei, D. Srivastava, B. J. Garrison, *Surf. Sci.* **374**, 333 (1997).
- M. Enachescu *et al.*, *Tribol. Lett.* **7**, 73 (1999).
- D. S. Grierson, E. E. Flater, R. W. Carpick, *J. Adh. Sci. Tech.* **19**, 291 (2005).
- R. W. Carpick, D. F. Ogletree, M. Salmeron, *J. Colloid Interf. Sci.* **211**, 395 (1999).
- B. Luan, M. O. Robbins, *Nature* **435**, 929 (2005).
- B. Luan, M. O. Robbins, *Phys. Rev. E* **74**, 26111 (2006).
- U. D. Schwarz, O. Zworner, P. Koster, R. Wiesendanger, *Phys. Rev. B* **56**, 6987 (1997).
- G. Gao, R. J. Cannara, R. W. Carpick, J. A. Harrison, *Langmuir* **23**, 5394 (2007).

- J. N. Israelachvili, *Intermolecular and Surface Forces* (Academic Press, London, ed. 2, 1992).
- A. V. Sumant *et al.*, *Adv. Mat.* **17**, 1039 (2005).
- F. S. Bates, G. D. Wignall, W. C. Koehler, *Phys. Rev. Lett.* **55**, 2425 (1985).
- M. J. Brukman, thesis, University of Wisconsin–Madison, Madison, WI (2005).
- B. N. J. Persson, E. Tosatti, D. Fuhrmann, G. Witte, C. Woll, *Phys. Rev. B* **59**, 11777 (1999).
- R. E. Walkup, D. M. News, P. Avouris, in *Atomic and Nanometer-Scale Modification of Materials: Fundamentals and Applications*, P. Avouris, Ed. (Kluwer, Dordrecht, Netherlands, 1993), p. 100.
- X. Zhao, M. Hamilton, W. G. Sawyer, S. S. Perry, *Tribol. Lett.* **27**, 113 (2007).
- M. R. Sørensen, K. W. Jacobsen, P. Stoltze, *Phys. Rev. B* **53**, 2101 (1996).
- G. A. Tomlinson, *Philos. Mag.* **7**, 905 (1929).
- J. A. Harrison, C. T. White, R. J. Colton, D. W. Brenner, *Thin Solid Films* **260**, 205 (1995).
- We thank J. Butler and J. Yang for loaning and polishing the (001)-oriented single-crystal diamonds and for helpful advice regarding H termination. J. Harris supplied (111) single-crystal diamonds used as references in the SFG measurements. We also thank L. Bruch for extensive discussions and B. Gotsmann for a helpful reading of this manuscript. Supported by the NSF CAREER Award no. CMS 0134571; an NSF Graduate Research Fellowship; and the Air Force Office of Scientific Research, grant FA9550-05-1-0204.

Supporting Online Material

www.sciencemag.org/cgi/content/full/318/5851/780/DC1
Materials and Methods
SOM Text
Fig. S1
References

9 July 2007; accepted 21 September 2007
10.1126/science.1147550

A Predictably Selective Aliphatic C–H Oxidation Reaction for Complex Molecule Synthesis

Mark S. Chen and M. Christina White*

Realizing the extraordinary potential of unactivated sp^3 C–H bond oxidation in organic synthesis requires the discovery of catalysts that are both highly reactive and predictably selective. We report an iron (Fe)-based small molecule catalyst that uses hydrogen peroxide (H_2O_2) to oxidize a broad range of substrates. Predictable selectivity is achieved solely on the basis of the electronic and steric properties of the C–H bonds, without the need for directing groups. Additionally, carboxylate directing groups may be used to furnish five-membered ring lactone products. We demonstrate that these three modes of selectivity enable the predictable oxidation of complex natural products and their derivatives at specific C–H bonds with preparatively useful yields. This type of general and predictable reactivity stands to enable aliphatic C–H oxidation as a method for streamlining complex molecule synthesis.

The 20th century witnessed tremendous advances in synthetic methods and strategies that have enabled small molecule targets of extraordinary complexity and biological importance to be synthesized in the laboratory (1). An important remaining challenge is to achieve syntheses with heightened levels of

efficiency. Because many biologically relevant small molecules are oxidized hydrocarbons, reactions that incorporate oxidized functionality selectively into organic frameworks are of particular interest in this regard. Three general reaction classes have been developed for this purpose: functional group interconversions, C–C bond-forming reactions of preoxidized fragments, and olefin oxidations. With these reactions, modern synthetic planning often centers around the use and maintenance of preexisting oxidized functionality. A powerful new class of reactions is

emerging that introduce oxidized functionality directly into aliphatic (sp^3) C–H bonds. Oxidation reactions for isolated, unactivated sp^3 C–H bonds capable of operating with predictable selectivities on complex substrates hold special promise for streamlining syntheses. Such reactions would provide a general way to install oxidized functionalities at a late stage, thereby reducing unproductive chemical manipulations associated with carrying them through a sequence (2, 3).

Despite important advances in the discovery of catalytic methods for aliphatic C–H bond hydroxylations, aminations, and alkylations (4–6), selective reactivity with complex substrates has only been demonstrated for activated C–H bonds (i.e., adjacent to a heteroatom or π system) (7–11) or via the use of substrate directing groups (12–14). High-yielding oxidations of isolated, unactivated sp^3 C–H bonds are rare, and predictable reactivity has only been shown with simple hydrocarbon substrates (10, 15–17). The paradoxical challenge in solving this problem lies in discovering a catalyst that is both highly reactive and predictably selective for oxidizing these inert and ubiquitous C–H bonds. Moreover, to be useful in complex molecule synthesis, this reactivity and selectivity must be general for a broad range of densely functionalized substrates. Nature's design principles for creating such catalysts involve the use of elaborate protein binding pockets that inherently limit substrate generality. A different

Department of Chemistry, Roger Adams Laboratory, University of Illinois, Urbana, IL 61801, USA.

*To whom correspondence should be addressed. E-mail: white@scs.uiuc.edu